VOL. 9, NO. 5, MAY 2014 ISSN 1819-6608
ARPN Journal of Engineering and Applied Sciences


www.arpnjournals.com

KERS APPLICATIONS TO AEROSPACE DIESEL PROPULSION

Luca Piancastelli[1], Leonardo Frizziero[1] and Eugenio Pezzuti[2]
[1]Department of Industrial Engineering, Alma Mater Studiorum University of Bologna, Viale Risorgimento, Bologna, Italy
[2]Faculty of Engineering, University of Rome Tor Vergata, via Del Politecnico, Rome, Italy
E-Mail: leonardo.frizziero@unibo.it

ABSTRACT

Surprisingly, the safety of a flight is still not guaranteed to maximum steam ejection of power during take-off. Moreover, modern aircraft require significant amounts of electricity. It could also be argued that today in many respects the automotive industry appears to be a technology leader with respect to the aerospace industry that, instead, is more conservative. Ferrari has developed, and implemented, on their F1 cars, an electronic device, called KERS, which is able to produce electricity, with peaks of 60 KW for 7s, with a mass of 20 kg, including rechargeable batteries. The main goal of this paper is to explore utilization of turbo-charged aerodiesel engines and conduct feasibility study of the F1-derived KERS to assist power generation in normal and critical flight phases. The KERS' reversible brushless electric motor works as a generator for all aircraft power needs and also provides starting power. It is demonstrated here that such design philosophy improves performance and flight safety of light-to-medium airplanes and helicopter.

Keywords: diesel engine, hybrid aircraft, kinetic energy recovery system, li-ion battery systems, turbine engines.

1. INTRODUCTION

As surprising as it may sound the racing automotive technology is ahead of aerospace industry in many technical areas with bold innovations and new implementations. One of the chief reasons is that aerospace industry is rather conservative and relies on proven technology primarily for safety reasons [1-5]. Automotive leads aerospace industry in many advanced technological applications, such as widespread utilization of CFRP, modern piston-engine designs, hybrid systems, and KERS.

In the research work only OTS design solutions are considered. The likely future improvements are not discussed or utilized as only state-of-the-art data are available and realistically achievable today. The automotive experience in this particular area is discussed.

We first introduce some important Li-ion battery management considerations in addition to discussing the reliability issues of modern battery systems. Brief consideration of modern electrical motors/generators is introduced. Different propulsion options and systems are analysed. A fully electric aircraft is explored [4]. A propeller-powered airplanes and powered rotorcraft with KERS are used as examples. An AB 212 aerodiesel+KERS engine replacement is analyzed as an example for helicopter applications. The turboprop airplane of choice is a Pilatus PC-6 for which aerodiesel+KERS engine replacement was studied. We will demonstrate in the subsequent text how diesel+KERS re-engined aircraft in many respects offer improved flight safety, lower operating cost, and get better flight performance figures.

2. POWER PLANT AND BATTERY MANAGEMENT SYSTEM

For the purpose of this article we consider the power plant to be an assembly of the propulsion device (s), the engine (s), the speed reducer (s) and the energy storage system (s). For example, the helicopter power plant may consist of the turboshaft (engine), the main rotor blades (propulsion device) and the energy storage system (s) incorporating fuel tanks and electrical batteries [4]. Similarly a turbine-propeller airplane will consist of one or more turboprop engines, reduction gearing (torque converters), propeller and fuel tanks with associated electrical system that is required not only to support engine operation but also increasingly more aircraft systems [4]. A powerplant also includes accessory drives necessary for start-up, FADEC or engine control, auxiliary systems, and the electrical generators as aircraft electric power system (s) sources [4].

2.1. Batteries

Battery reliability is a major issue for every aircraft and associated powerplant (s). Even with common and well proven lead-acid batteries reliability Figures are not always satisfactory [4]. On the other hand, common aviation Ni-Cd batteries have some serious thermal-runway issues despite having many favourable power and capacity characteristics [4]. As an example of current battery problems, we show the statistics from the German highways where the most common vehicle breakdown was due to malfunctioning battery (shown in Table-1).

Table-1. Batteries are the most common cause of failures in cars thus requiring road assistance. Source: ADAC 2008. Germany.

Percentage of failure	Cause of failure
52%	Battery
15%	Flat tire
8%	Engine
7%	Wheels
7%	Fuel injection
6%	Heating, cooling
5%	Fuel systems

The advantage of Li-ion batteries in terms of high power-density and low mass/weight is so essential that their utilization is highly recommended in aeronautics and aerospace vehicles where high power-to-weight (and power-to-volume) ratios are fundamental.

However, the risks of the new battery technologies are substantial as demonstrated by Boeing 787 "Dreamliner" recent problems. Li-ion batteries also have had their share of problems in laptop computers and in smart-phones prompting expensive recalls. Safety concerns are on the rise for this type of products as reported in [6, 7].

In automotive industry, extensive tests have been made on F1 (Formula 1) KERS battery to reach satisfactory reliability, power-density, and safety. Several accidents have paved the way and forced an in-depth understanding with important experience gained. For example, F1 race cars experienced multiple fire and electric shock accidents in the past prompting extensive redesigns. Clearly, any uncontained fire is the most serious hazard in any manned vehicle and especially so for airborne passenger-carrying aircraft.

2.1.1. Li-Ion cell characteristics

In a discharging Li-ion cell, lithium is ionized in a (typically) graphite anode. The Li ions move in an electrolyte to penetrate through a separator and to a cathode. In this way the charge flow is achieved. In a reverse flow, the charging process brings the Li ions from the cathode to the anode. Cell temperature and cell voltage depend on many factors. The preservation of optimum operating conditions for Li-ion cells is a critical requirement for the battery-management system.

At temperatures above 100°C, the electrolyte begins to break down, releasing gases that can cause pressure to build within cells designed without pressure-relief mechanisms. At high enough temperatures, Li-ion cells can experience thermal runaway (rapid overheating) as oxides break down, releasing oxygen, which further accelerates the temperature increase. Mechanical fatigue is present during each cycle [8, 9, 10].

Vehicle's g-loads also affect the battery integrity. The result of such stresses may be immediate or induce veiled creep. Creep reduces the battery capacity and when the cracks grow large enough the physical integrity of the battery may be at risk. The final battery failure may be associated with the uncontained temperature rise and possibly fire. The timing of this event is random and it can happen at any time. Careful monitoring of the battery performance is necessary.

Another important issue for safe battery operation is its ability to withstand high g-loads. The best battery configuration known to combat g-loads is the pouch cell as shown here in Figure-1. This cell configuration is resistant for loads normal to the plane of movement while maximum in-plane loads should be limited to reasonable levels (see [6]). The pouch cell should be protected from humidity and puncturing.

Commonly in an F1 KERS the battery pack is cooled by the engine's cooling system and is protected by a rigid casing. A typical arrangement as used by Mercedes Benz is shown in Figure-2. The pouch cells are arranged horizontally to prevent fatigue shock from vertical acceleration. All the components are liquid cooled. Protection against swelling is achieved with a flexible envelope as shown in Figure-3. The immersion in a liquid coolant has several advantages: a direct control of cell temperature and the possibility to cool down the battery during very fast charging and discharging. The enclosure protects the battery against punctures and contains the battery in case of total failure. The mounting technique of the cells reduces g-loads. Composites are used to reduce weight by keeping strength [11].

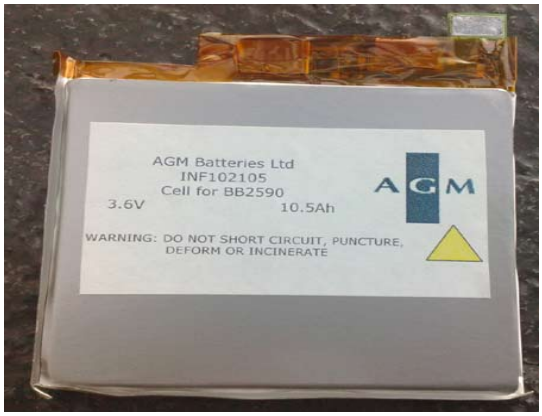

Figure-1. The pouch cell offers simple, flexible and lightweight solution to battery design. Exposure to high humidity and temperatures shorten service life. Courtesy of Cadex [12].

Rapid charging requires the avoidance of the saturation part of the charge as shown in Figure-6. Initially the applied voltage should be reduced to avoid overcharging and excessive temperature increase. This is the main reason why full battery discharge should be avoided. During an optimized charging process the maximum amount of energy is supplied during the first hour. Afterward charging takes place with reduced energy accumulation. For ideal cycling the battery should work between 25% and 75% charging levels. This means that only 50% of the effective capacity is practically available at a time. It is possible to use the full capacity of a battery cell, but at a price: in this case mechanical fatigue, charging current, SOC, large input/output voltage variations and, as always, temperature should be accurately monitored to avoid battery self-destruction. Another typical problem is the calibration of the battery cell. The full discharge/charge condition changes with the cell life and is shown in Figure-7. Calibration is achieved by applying a full charge, then discharge, and then a repeated charge. This is done with battery installed or with a special battery analyzer as a part of battery maintenance procedure.

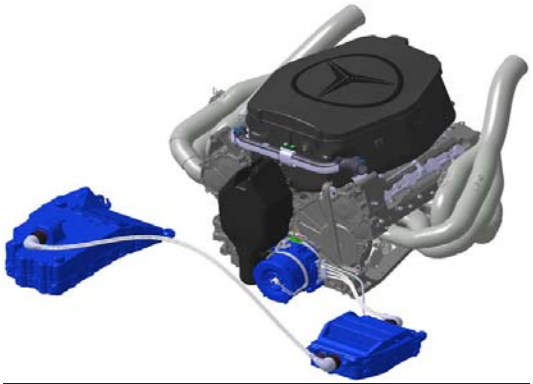

Figure-2. The KERS of Mercedes F1 (blue colored) is composed of the motor/generator (center) connected to the crankshaft, the PCU (right), and the battery pack (left).

Figure-3. Swelling can occur as part of gas generation. The reasons for that are still not fully understood. Courtesy of Cadex [12].

The cell capacity is severely reduced by the charge/discharge cycle frequency as clearly illustrated in Figure-4. A pool of new 1500 mAh Li-ion batteries for smartphones was tested in a Cadex C7400 battery analyzer. All pouch packs showed a starting capacity of 88-94% and decreased in capacity to 73-84% after 250 full discharge cycles. The battery cell capacity is also reduced by the excessive voltage charge as shown in Figure-5 and reported in [13].

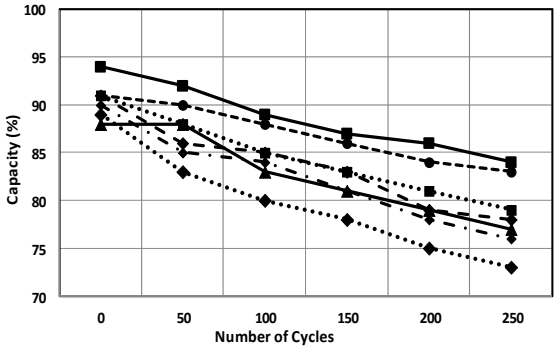

Figure-4. Capacity decreases with charge cycling frequency. Courtesy of Cadex [12].

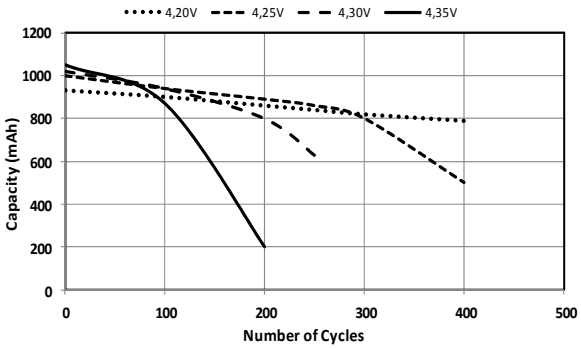

Figure-5. Effects on cycle life at elevated charge voltages. Higher charge voltages boost capacity but lower cycle life and compromise safety.

For example, in F1-KERS applications, charging occurs during vehicle's (dynamic) braking and is very short. Also discharging time is very limited (7s). This further limits battery life (see Figure-8). Fortunately, the F1-KERS the battery management is simplified by the limited capacity of the battery stack and by the short life-span of the system.

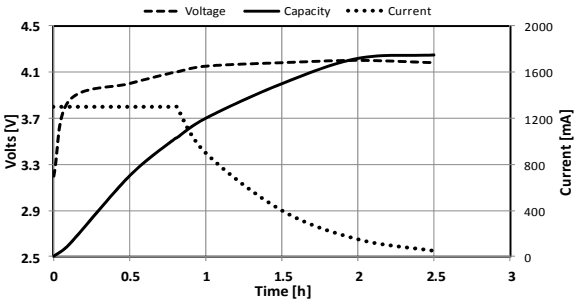

Figure-6. Capacity as a function of charge voltage (Li-ion battery). Courtesy of Cadex [12].

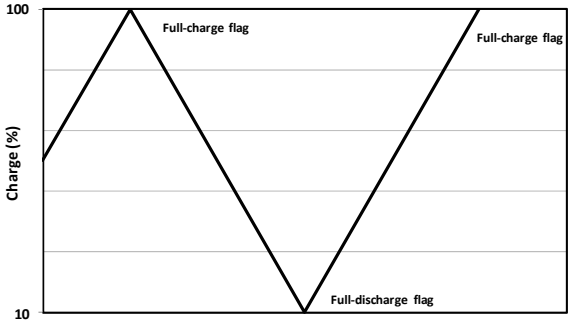

Figure-7. Full-discharge and full-charge flags. Courtesy Cadex [12].

2.1.2. An example: The Chevrolet colt battery management system

The management system of a hybrid vehicle ensures the safety and reliability of the multi-cell lithium-ion battery stack which delivers power to the drive system.

The battery management system is composed of battery-monitoring boards that use two independent subsystems to monitor battery cell health and deliver digital results to a host processor that controls the system operation. An opto-electronic signal interface ensures isolation between the high-voltage battery-sensing circuitry and control ECUs.

In a Chevrolet Volt hybrid vehicle, the battery performance is obtained by the multi-board digital electronic design (see Figure-9) that manages a system responsible for the optimization of the range, performance, endurance and the overall safety of the Li-ion battery pack.

Since a Li-ion cell maintains nearly flat voltage output across the middle of its capacity range, SOC and temperature should be accurately monitored. SOC monitoring is difficult for Li-ion cells and current-based or voltage-based methods are typically used for it.

In Chevy Volt's SOC monitoring and controlling of Li-ion cells requires a high speed CPU. Each sensing subsystem has a pair of L9763 ASIC with a Freescale S9S08DZ32 40-MHz HCS08 MCU packing internal 32-kbyte flash, 2-kbyte RAM, and 1-kbyte E2PROM on-chip as illustrated in Figure-10. An external 4-MHz clock is used for the MCU.

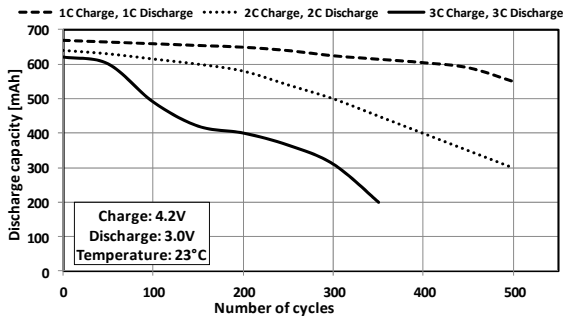

Figure-8. Cycle life of Li-ion with cobalt cathode at varying discharge levels. The wear-and-tear of a battery increases with higher loads [13].

"The Chevy Volt battery pack consists of 288 prismatic Li-ion cells which are in turn packaged into 96 battery-cell groups to deliver a system voltage that the analysts measured at 386.6 VDC. Those battery-cell groups are equipped with the temperature sensors and cooling elements in four main battery modules. Voltage-sensing lines attached to each cell group terminate in a connector on top of each battery module, and a voltage-sensing harness joins the connector to a battery-interface module that sits on top of each battery module. Here, four colour-coded battery interface modules operate at different positions in the battery stack, corresponding to low, medium, and high voltage ranges of DC voltage offset for the set of four modules. Data from the battery-interface modules moves upstream to the battery-energy-control module. That module in turn passes fault conditions, status, and diagnostic information to the hybrid-powertrain-control module, which serves as the host controller for vehicle level diagnostics. At any time, the overall system runs more than 500 diagnostic events every tenth of a second; 85% of those diagnostic runs focus on the battery-pack safety, and the remainder target battery performance and life" [14].

Figure-9. The battery-interface control module is composed of the red, blue, and green boards shown above in the second column from the right. (Courtesy of UBM TechInsights).

It should be noted that this system is tuned to keep the battery stack within the area of low voltage drop (see Figure-11). Temperature control is critical in this range.

2.1.3. Aircraft battery operation

The aircraft battery management system is complicated and contains many components [15, 16]. Battery is safety critical component. When failure occurs, the temperature and the internal pressure rise in a nonlinear fashion resulting in a high probability of fire. For reliable and certified aircraft operation redundancy is mandatory. Dual redundancy may suffice for ECUs, and at least triple sensor redundancy is needed. A critical battery-safety issue is cooling. Warming up of battery is a nonlinear process with overheating possibly occurring very rapidly. Cooling power has to be sufficient to arrest thermal runaway and the containment should prevent damage expansion and fire propagation. Redundant automatic fire detection and suppression systems have to be installed [4]. Venting should be provided for smoke removal. Such "accessories" significantly adversely affect the power-to-weight ratio of the battery stacks.

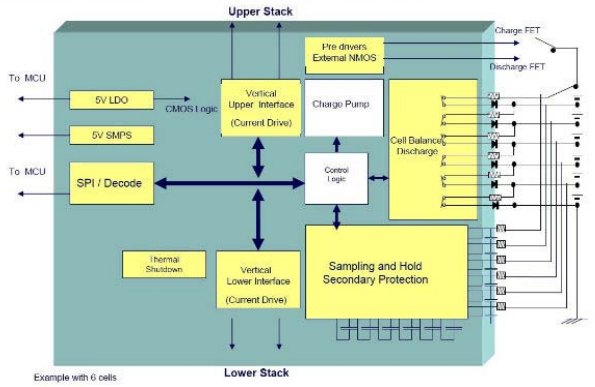

Figure-10. The L9763 ASIC includes on-chip circuitry for measuring voltage and current from Volt cell groups as well as for balancing charge in those cells through passive resistive cell-balancing techniques. Courtesy of STMicroelectronics [14].

For example, the 2011 F1 McLaren-Mercedes KERS lithium-ion battery pack has a mass of 14.7 kg (32.4 lb) and costs about $96, 000. The battery pack is replaced or reconditioned more than once each race week [11]. Since a 2011 F1 KERS could produce 400 kJ (F1 regulations for the year 2011). The energy density of the F1-KERS pack is:

$$\text{Energy Density} = \frac{400}{14.7} = 27 \quad [\text{kJ/kg}] \qquad (1)$$

This pack includes the battery management system, but the mass figure is without the coolant. KERS's battery pack "survives" about 1,000 charging/discharging cycles. The in plane acceleration (horizontal acceleration) should not exceed 1, 500 cycles at 6-g. Vertical (bouncing) acceleration is less critical but should not exceed 10-g. To achieve the necessary reliability for passenger aircraft operations the energy density should be cut in half, i.e., achieve 14 [kJ/kg]. Luckily in a commercial passenger aircraft such high acceleration levels are never reached in normal operations. The battery management system has already sufficient reliability to be Title 14 CFR (FAR) certified in USA.

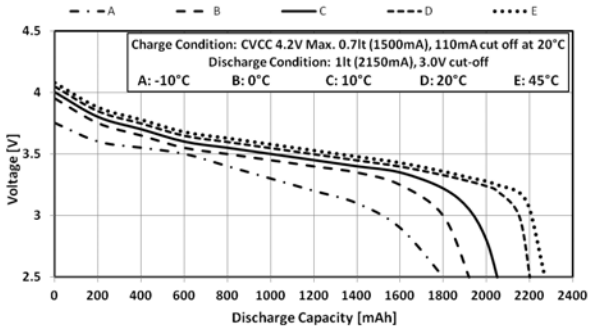

Figure-11. At a given temperature and discharge current level, a Li-ion cell such as this Panasonic CGR18650CG exhibits nearly flat output voltage in the middle portion of its discharge range. This is an advantage for a power source but requires accurate SOC monitoring. (Courtesy of Panasonic).

Battery aging is also a critical factor. Li-ion batteries are stored at 40% charge level to minimize the spontaneous discharge [12]. For F1 KERS storage time should not exceed two years. For self-discharge, storage temperature is critical (see Table-2).

Table-2. Self-discharge per month of Li-ion battery at different temperatures and state-of-charge (SOC) [17].

Charge condition	**0°C** (32°F)	**25°C** (77°F)	**60°C** (140°F)
Full charge	6%	20%	35%
40-60 % charge	2%	4%	15%

2.1.4. Battery environmental impact

Lithium-ion battery positive electrodes are made of materials that generate lithium ions, while the negative electrodes are of the elemental lithium intercalated on graphite [18]. Lithium ions are "widely distributed in nature; trace amounts are found in many minerals, in most rocks and soils, and in many natural waters," and FDA approves the use of ionic lithium in drugs [19]

Neither elemental lithium nor graphite is toxic, and their combination eliminates the volatile nature of metallic lithium. The electrolyte can be made out of different materials, but LiPF6 in carbonate solvent is the most common. Lithium carbonate can be a toxin to humans and animals, while LiPF6 can react with water to produce hydrofluoric acid, which is a major pollutant and contact poison. As of the moment, lithium-ion cells have the least negative environmental impact in the entire battery family.

An electric aircraft is conceptually simple and not particularly difficult to design and manufacture with OTS components. An example of that will be given in the following paragraph. However, the performance of electric prime mover is not competitive with the traditionally powered aircraft. Batteries are still too heavy and do not deliver acceptable and expected ranges or endurance.

3. AUTOMOTIVE TURBO-DIESEL CONVERSION

Automotive turbo-diesel was conceived for high torque at low rpm applications and for stringent Euro-4 emissions. The power and mass data for some automotive conversions (into aeroengines) is depicted in Figure-12. We show the torque-rpm curve of a 1300 jtd common-rail turbo-diesel engine in Figure-13. In this particular engine a "small" turbocharger was installed to reduce turbolag and to further improve torque characteristics at low rpm. The same engine with a proper tuning may reach performance curves shown in Figure-14. In this case the calculated airbox pressure is 1.45 bar. To obtain the power curve of Figure-14, the ambient pressure should be kept at the target altitude.

If an aircraft cruise altitude is 10,000 m ISA+0 or about 33,000 ft, the atmospheric pressure is 0.264 bar (about 3.9 psi). The necessary compression ratio for the air-intake turbo-charging system is:

$$PR = \frac{p_{airbox}}{p_{10,000}} = \frac{1.45}{0.264} = 5.5 \quad [-] \qquad (2)$$

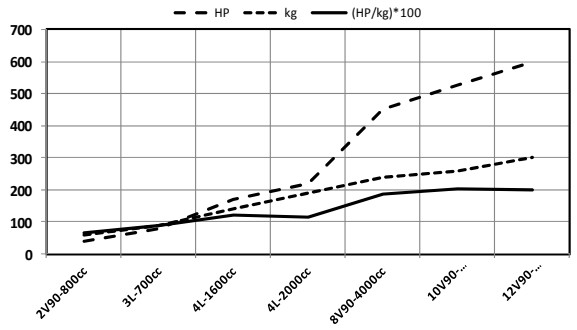

Figure-12. Turbo-diesel power and mass data at sea level.

And the mass flow is increased by a factor:

$$MassFlow_{ratio} = \frac{\rho_{SL}}{\rho_{10000}} = \frac{1.225}{0.41} = 2.96 \quad [-] \qquad (3)$$

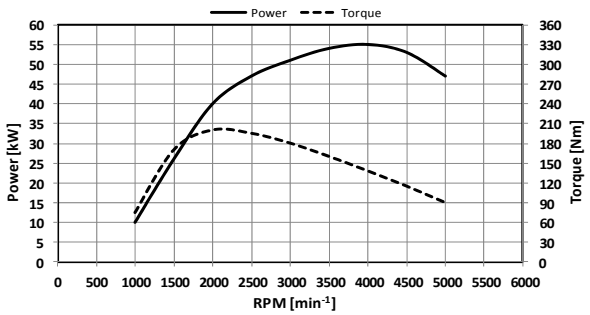

Figure-13. Power/Torque rpm curves for 1300 jtd diesel engine.

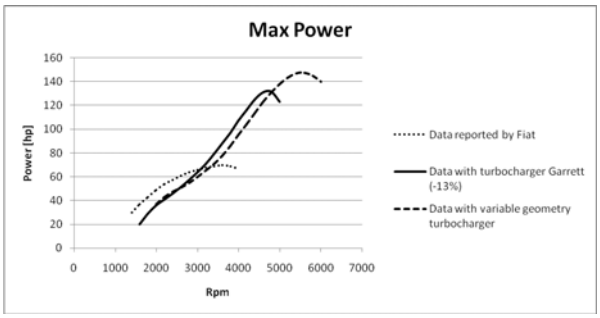

Figure-14. Power vs rpm for the 1,300 jtd Euro0 aircraft engine. Red line is the original power curve (automotive Euro4); blue and yellow are the aircraft installed power curves (Euro0) at two different settings.

A second larger turbocharger with a nominal mass flow multiplied by a factor 2.96 should be added. Smaller turbocharger will work at SL and the second turbocharger will start at a predetermined altitude. Such twin system is analogous to an arrangement of the vintage Rolls Royce Merlin 61 (two-stage turbo-charging with intercooler). The main difference is that turbocharger's compressors are not driven by crankshaft (as in superchargers) but by mated exhaust gas-operated turbine. The turbocharger improves engine efficiency by recovering part of the energy from exhaust gases still at high temperature. The exhaust gas temperature (750°C) is converted into dynamic pressure in the turbine which powers the intake air compressor attached on the same spool. The high turbo charging pressure does not affect SFC which is usually very good (150 gr/HP-h), but affects the overall weight. The second-stage turbocharger for the 1300 jtd engine adds about 15 kg to engine mass, without any improvement in output power. The advantage is that SFC remains almost constant for all output levels (see Figure-15).

The efficiency of common-rail turbodiesel is slightly affected by altitude and outside temperature. However, a "critical altitude" exists at which full throttle is applied and turbocharger gives maximum performance. Above the critical altitude the power output decreases as in normally-aspirated engines even with full throttle applied. If the power output is reduced, the turbocharger(s) will slow down. To recover full turbocharger speed and full rated engine power the aircraft's only option is to descend into denser air [20].

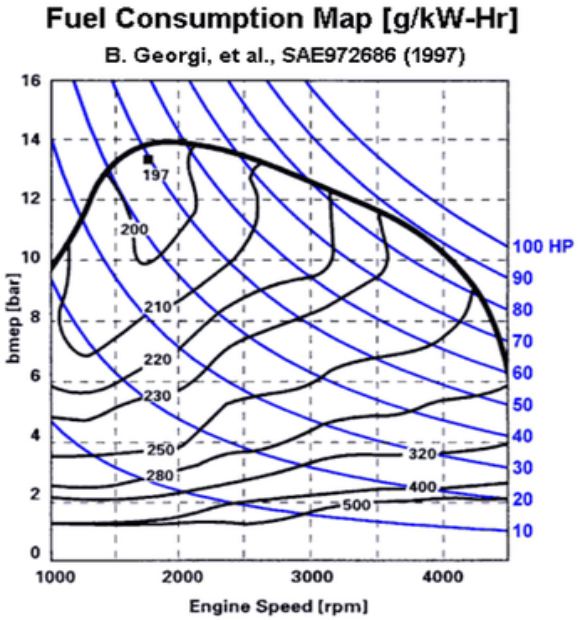

Figure-15. SFC for turbo-diesel. The fuel consumption is approximately constant for every practical working set point [21].

4. DIESEL VERSUS TURBINE AEROENGINE

Turboshaft, turboprop, turbofan (ultra-high, high, medium, and low bypass ratios), and, now almost extinct, pure turbojet gas-turbine engines are open systems incorporating rotating turbomachinery and function by continuously processing air and creating thrust in the nozzle and/or torque on the rotor/propeller shaft [1, 2, 3, 5, 22, 23]. Turbine engines are workhorse in civil and military aviation today which spans everything from the VLJ and helicopters to heavy commercial high-bypass turbofan airplanes (B747, A380) and heavy-lift helicopters [1-3]. In a simple way, turbine engines create thrust and/or torque on the shaft by accelerating air volume per unit time at a certain spool rpm. The fuel flow depends on the air mass flow rate and must be carefully monitored and controlled [5, 22, 23]. In the old turbojet engines a 3D camshaft regulated the fuel flow for temperature and altitude compensation. In modern turbofan engines dual-channel FADEC calculates the fuel flow for transient and steady-state operations, controls a number of engine parameters while protecting working envelope from exceeding design limits, such as overheating (exceeding EGT/ITT/TIT), over-speeding (maximum spool RPMs), and over-boosting (maximum combustor pressure) [2]. FADEC is throttle-by-wire control of the fuel flow (and many other parameters) based on the thrust request set by operator/pilot using the thrust/power/torque (and condition and propeller when appropriate) levers [2]. In the past the fuel flow could be controlled manually by the pilot through a mechanical lever, but such system does not exist in modern FADEC-equipped turbine engines where digital electronics with controlling software has the full authority over engines. The turbine engine is conceptually simple.

However, the control and the design are truly complicated requiring expensive temperature- and fatigue-resistant alloys, precision machining, and high-quality costly certified components. Turbine engines of today are extremely reliable also because large amount of money has been invested in their development and testing and so much has been learned in the past 60+ years. However, turbine engines do have some serious weaknesses where, for example, aero-diesels stand out. Some of the deficiencies of turbine engine designs are their relatively high SFC, susceptibility to FOD, high purchasing cost, compressor stalls and inlet flow instabilities, and essentially being normally aspirated. Only at design set point has the turbine engine competitive SFC and they work best at nominal thrust/power settings. Turbine's SFC decreases and specific thrust increases by increasing compressor PR and TIT [5, 22, 23]. But that requires expensive heat-and stress-resistant hot-section materials and efficient blade-cooling designs while simultaneously providing ACC and other internal gas flow control mechanisms [1-3].

Power output or thrust of jet engines depends almost linearly on air density. For example, at 6662 m ISA+0 (21, 000 ft), the maximum SL thrust output will be approximately halved. This is chiefly due to the fact that air density is halved from SL ISA 1.225 to 0.6125 [kg/m^3] at 6662 m ISA [24].

On the other hand, turbo-diesel's power output depends on the air density in the airbox. The intake pressure can be partially recovered by the turbo-charging (turbo-normalizing) system and the temperature kept constant and relatively low by intercooler(s). The cooling system provides additional thrust by Meredith's effect [25]. A turbo-charging system increases the engine installation mass.

For the most powerful automotive turbodiesel aero-conversion (600 HP or 441 kW at 300 kg) discussed here, the maximum available air-intake pressure ratio (PR) is 5.6:1. The pressure in the airbox must be kept at 1.88 bar minimum. So the necessary minimum intake PR determines minimum required outside pressure (and critical altitude) to achieve full power:

$$p_{outside\,min} = \frac{p_{airbox}}{PR_{max}} = \frac{1.88}{5.6} = 0.33 \quad [\text{bar}] \qquad (4)$$

This ambient pressure corresponds to 8,400 m (27, 500 ft) ISA+0 (critical or recovery density altitude). Simultaneously, at this density altitude, a typical modern turbofan will produce roughly only one-third to two-fifths of the SL thrust/power.

5. KERS MOTOR/GENERETOR

A typical F1 KERS motor/generator has a mass of about 5 kg and a power output of 60 kW (80 HP) for about 7 seconds (energy of 420 kJ). This extraordinary result is achieved at rpm range of 10,000 up to 17, 000. The power-to-mass ratio (PD) is 12 kW/kg. This is a very

high value when compared with the data shown in Figure-12. However, a power conversion unit (torque converter) should be added with a mass of about 4.5 kg. Also additional wiring harnesses of about 1kg are needed. The actual engine power-density without associated fuel tanks is accordingly:

$$PD_{F1-KERS} = \frac{\text{Power}}{\text{Engine Mass} + \text{Controller Mass} + \text{Wiring Mass}} = \quad (5)$$
$$= \frac{60}{5+4.5+1} = 5.7 \quad [\text{kW/kg}]$$

Compared to regular electric/generators this Figure is quite good. It is however, possible to find today an OTS air-cooled, ironless, brushless, 40 kW motor/generators with a mass of only 12 kg. The motor power density for such system is:

$$PD_{OTS} = \frac{\text{Power}}{\text{Engine Mass} + \text{Controller Mass} + \text{Wiring Mass}} = \quad (6)$$
$$= \frac{40}{12+4+1.2} = 2.32 \quad [\text{kW/kg}]$$

This is still a respectable value. Such motor/generator runs at 6000 rpm and can replace both the alternator (AC generator with DC rectifier) and the DC starting motor [4]. A visual display of such installed motor/generator on a stock 1300 jtd turbo-diesel is depicted in Figure-16. In the case of a diesel-engine (prime mover) total failure, such electric motor can still provide emergency power. The electric motor also provides assistance during the startup-shutdown phases of the engine-propeller combination [26].

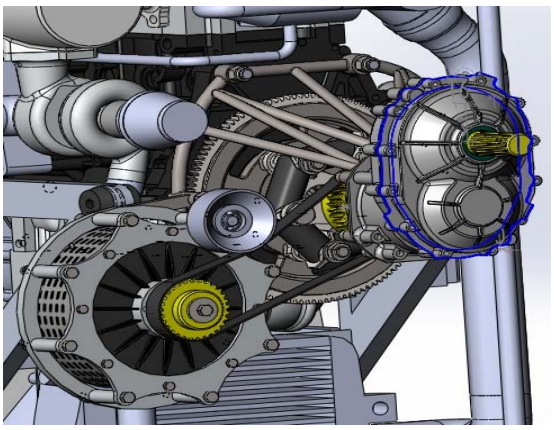

Figure-16. The 40kW motor/generator is connected to the propeller shaft through a timing belt.

5.1. Small diesel with KERS: the 1600 jtd case study

For this case study, the original battery, the generator, and the starting motor were removed from the powerplant assembly. These components were replaced with the KERS. An OTS motor/generator is connected to the propeller with the timing belt, the power control system and the battery (see example in Figure-16). The motor/generator and the PCS are all air-cooled, while the battery stack is chosen based on the F1 racing experience. The pouch cells are controlled by a separate power management system and water-cooled. A detonation-proof box contains the Li-ion cells damping the horizontal accelerations. Since the motor operating voltage is high (600 VDC) the electrical harnesses are short. The aerodiesel+KERS powerplant is installed behind the bulkhead. Mass breakdowns of such designs are summarized in Tables 3 and 4.

The additional weight required for a peak power of 40 kW of 5 seconds duration is 20 kg (Additional Mass = 33.9-15 ≈ 20 kg). The 1600 jtd aircraft aero-engine version has a mass of 145 kg and a power output of 170HP (125kW). With the KERS, the 1600 jtd mass is increased to 154 kg with the peak power output of 224HP (165 kW). For comparison, the 2000 jtd aircraft engine has a mass of 195 kg at a power output of 220 HP (161kW), or basically is 41 kg (90 lb) heavier for the same peak power output. The 1600 jtd diesel+KERS have additional advantage of having larger generator (20kW). The original automotive generator delivers only 1kW peak power.

Another advantage that KERS offers is the ability to quickly start and stop the propeller (and the engine) with the full authority of the 40 kW (55 HP) electric motor. Such starting power is an order of magnitude larger than in common DC starter motors and should offer superior performance under all-weather conditions. Additionally, this improves engine TBO and significantly reduces maintenance cost. Unfortunately, current cost of the Li-ion battery stacks is still prohibitive (US$ 90, 000+). In the power balance of diesel and KERS multi-objective optimization can be used [27, 28, 29].

6. AERODIESEL+KERS REPLACEMENT FOR THE AB 212 HELICOPTER

An Italian-version (Agusta-Bell) AB 212 medium-helicopter with two turboshafts generate maximum takeoff power of 1500 SHP (1800 SHP maximum for time-limited operation) de-rated due to gearbox torque restrictions. Single engine cruise at full weight requires continuous 765 HP at SL ISA while single-engine 30-minute rating is 900 SHP. The internal AB 212 fuel capacity is 720 kg (1584 lb). The turboshaft twin power-pack has a mass of 340 kg. An aerodiesel+KERS replacement is achieved by 2 x 600 HP turbo-diesel units plus 2 x 150 HP electric (KERS) motors/generators. The maximum continuous cruise power available is thus 1200 HP, while the AB 212 helicopter requires 1050 HP at normal cruising speed at full weight (about 5100 kg) and SL ISA. The aerodiesel engines in this configuration halve the SFC of the original turboshaft (P and W PT6T-3B). The internal fuel tanks may be reduced by 360 kg, thereby increasing the useful load. However, the aerodiesel power-pack is heavier. The total mass is 300 kg for each engine, while the KERS system (from F1 data: 80 HP at 26 kg) has a mass:

$$M_{KERS} = \frac{M_{F1}}{P_{F1}} \times P_{KERS} \times SF = \frac{26}{80} \times 300 \times 2 = 195 \quad [\text{kg}] \qquad (7)$$

Table-3. Automotive mass breakdown.

Item	**Mass** (kg)	**Notes**
Battery	7	Aircraft use
Battery	17	Automotive use
Generator	4.5	Automotive use
Starter	3.5	Automotive use
Total	15	With aircraft battery

Table-4. KERS mass breakdown.

Item	**Mass** (kg)	**Notes**
Li-Ion stack	14.7	F1 derivative
Motor/Generator	12	Commercial
PCS	4	Commercial
Belt assembly	2	Commercial
Wiring	1.2	Commercial
Total	33.9	

A derating (safety) factor SF of 2 was used for increased reliability. The aerodiesel+KERS power plant mass is thus:

$$M_{diesel+KERS} = 2 \times M_{diesel} + M_{KERS} = 300 \times 2 + 195 = 795 \quad [\text{kg}] \qquad (8)$$

The re-engined AB 212's MTOW is now:

$$MTOW_{diesel+KERS} = MTOW_{PT6-T} - M_{PT6-T} + M_{diesel+KERS} - M_{fuel} = \qquad (9)$$
$$= 5080 - 340 + 795 - 360 = 5175 \quad [\text{kg}]$$

This represents useful load reduction of 95 kg (210 lb) over the turboshaft-equipped AB 212 at SL. The payload will be thus reduced from 14 to 13 people fully equipped at SL ISA. However, an aerodiesel is turbocharged and will maintain SL-power theoretically up to 8400 m ISA. Turboshaft engine would only deliver a fraction of SL power at such altitude. For the cruise flight the continuous power is 765 HP, so the prolonged particular single aerodiesel operation is not possible at SL ISA. Single aerodiesel operation is only possible for 1 min. with the power boost of 680 HP. However the KERS will assist the pilot with 300 HP for 6s in the case of normal operation and 300 HP for the whole 12s in the case of emergency. This provides significant flight safety advantage.

Helicopter rotors have significant rotary inertia and a lot of torque/power is necessary to start it. In smaller helicopters the engine must be started first to reach idle speed and then generate power necessary to start rotor rotation. Free-turbine turboshafts are ideally suited for this task as the coupling with the power-turbine connected to the main rotor through transmission is achieved by hot gases only (or "gas-dynamic coupling"). The KERS electric motor can also assist aerodiesel prime mover during rotor startup. During shutdown KERS will be used in reverse role to charge batteries simultaneously offering high resistance and slowing down main rotor quickly which is not possible in turboshafts without rotor brakes. Accordingly, the traditional disconnect system or the centrifugal clutch will be avoided with KERS although disconnection from prime mover must still be achieved in the case of helicopter emergency autorotations. Aerodiesel+KERS combination thus offers advantages in lower SFC, altitude operations, supply, and flight safety. Diesel fuel is far less flammable than JP4 or Jet (A1). Another advantage is the possibility to purchase and stock the diesel fuel in private airfields thus avoiding the transfer flights to airfields for refueling or uneconomical fuel tankering. KERS provides additional power for critical flight phases (abnormal and emergencies). However, the helicopter performance will be reduced both in terms of payload and for single engine operation, but only at lower DA. At higher density altitudes (say above 5000 ft) the twin aerodiesel+KERS will outshine turboshaft twin-pack for the same weight. Battery costs are still substantial and the KERS aerospace implementation requires further improvements and cost reductions, but the future looks bright for such alternatives [30, 31].

7. AERODIESEL+KERS REPLACEMENT FOR THE PILATUS PC-6/B2 H2 TURBO-PORTER TURBOPROP

The Pilatus PC-6 airplane is a very successful design with a single-engine turboprop and MTOW of 2800 kg. A fuel capacity is 515 kg and payload is 1000 kg (2200 lb). Pilatus PC-6 is equipped with a single Pratt&Whitney Canada PT6A-27. This turboprop has an output power of 680 ESHP or 500 kW and mass of 153 kg. Most of the thrust (90%) in turboprop design comes from the propeller-generated thrust (torque on propeller shaft) and a very small part from the jet nozzle thrust [24, 25, 26]. We also envision an aerodiesel+KERS conversion for this airplane and study feasibility of such replacement. In fact it is possible to obtain 680 HP power rating for 1 minute with a 600 HP aerodiesel discussed here. The additional time-limited power may be important in high-density altitude operations. Due to halved SFC, the fuel tank capacity is reduced to 250 kg (550 lb), while aerodiesel engine mass remains 300 kg. The powerplant replacement will reduce takeoff weight by 103 kg for the same useful load or useful load can be increased by 103 kg for the same MTOW of 2800 kg (6160 lb):

$$TOWdiesel = MTOW_{PT6A-27} - M_{PT6A-27} + M_{diesel} - M_{fuel} = \qquad (10)$$
$$= 2800 - 153 + 300 - 250 = 2697$$

Reduced TOW will result in improved STOL performance with a TOD reduced from the certificated 440m to [24, 32, 33]:

$$TODdiesel = \left(\frac{MTOW_{diesel}}{MTOW_{PT6A-27}}\right)^2 TOD_{PT6A-27} = \left(\frac{2697}{2800}\right)^2 440 = 408 \quad [m] \qquad (11)$$

By using F1-KERS with the weight savings, we obtain additional power:

$$P_{KERS} = \frac{P_{F1}}{M_{F1}} \times M_{KERS} \Big/ SF = \frac{80}{26} \times 103/2 = 158 \quad [HP] \qquad (12)$$

If KERS is used during takeoff to assist main powerplant this will theoretically further reduce TOD [27, 28] to:

$$TOD_{diesel+KERS} = \frac{HP_{PT6A-27}}{HP_{diesel+KERS}} TOD_{diesel} = \frac{680}{(680+158)} 408 = 331 \text{ [m]} \qquad (13)$$

This turbo-charged aero-diesel engine has a critical altitude of 8400 meters. Above 8, 400 m the power will be reduced approximately in proportion to the air density [24, 33, 34-36].

The theoretical improvements, both with the aero-diesel alone and with the aerodiesel+KERS combination, are quite noteworthy. Here, engine replacement will result in operating cost reduction, improved flight safety, and better overall performance. However, the cost of KERS is still too high as seen in the AB 212 feasibility study earlier. Nevertheless, the availability of extra 158 HP at any altitude even for short duration may be priceless from the flight safety point of view. Additionally, liquid cooled aerodiesels do not experience thermal shock problems as air-cooled piston engines. However, liquid-cooling for aero-engines is still a controversial issue with many pros and cons.

A short discussion of the engine/powerplant PD is in order. Although, the PD of the engine itself seems to prefer turbine-engines over aero-diesels, the consideration of its larger required fuel storage and the decrease of the net power/thrust with increasing density altitude must be also taken into consideration. Accordingly, turbine engines may have better efficiency at lower DA's, although this is not their best range of operation as they prefer high altitudes with low air temperatures. However, turbo-charging enables aero-diesels to maintain SL power even at high density altitudes thus providing better PD over turbine engines which are normally aspirated air-breathing propulsion devices. Also the better fuel efficiency does give some advantages to diesel engines too. KERS is an additional, often safety-critical, power-source that is especially suited to diesel engines although it can be theoretically used with any kind of engines [30, 31].

8. CONCLUSIONS

It is possible to transfer what has been developed during the experience of F1 with respect to the KERS device directly to aerospace vehicles, in particular for aircrafts, UAVs, helicopters and airships, through the downgrading of battery use.

With appropriate adjustment of the project, it is possible to greatly improve the security and the reliability of the battery. As demonstrated, the aerodiesel+KERS combination is quite feasible for aircraft operations while improving flight safety and performance. However, the current battery cost is still prohibitive. More widespread commercial use will probably have to wait for technologically mature, lightweight, and cheaper battery systems. For specialized operations where flight safety is paramount and the cost is secondary, an aerodiesel+KERS combination offers distinct advantages already today. Diesel-powered aircraft is a realistic alternative to traditional aerospace propulsion systems both from the safety and the performance aspects. However, the reliability and robustness of water-cooled turbocharged common-rail aerodiesels still has to be proven and government's certifications obtained. AeroDiesel+KERS power-pack is apparently appealing solution for light-to-medium helicopters as it simultaneously improves flight safety and lowers operating costs. A slight reduction in performance is expected for low density-altitude operations only. For light-to medium size airplanes, the performance improvements look good in almost all aspects.

Nomenclatures

AC	Alternating Current
ACC	Active Clearance Control (Turbine engines)
ASIC	Application Specific Integrated Circuit
CFRP	Carbon Fibre Reinforced Plastic
CPU	Central Processing Unit
DA	Density Altitude [m]
DC	Direct Current
ECU	Engine/Electronic Control Unit
FADEC	Full Authority Digital Engine Control
FAR	Federal Aviation Regulations (USA)
EGT	Exhaust Gas Temperature [K]
ESHP	Equivalent SHP [kW], [HP]
FDA	Food and Drug Administration (USA)
FOD	Foreign Object Damage
ISA	International Standard Atmosphere
ITT/TIT	Interstage Turbine Temperature/Turbine Inlet Temperature [K]
KERS	Kinetic Energy Recovery System
M	Mass [kg]
MCU	Multipoint Control Unit
MTOW	Maximum Takeoff Weight/Mass [kg], [lb]
OTS	Off-the-Shelf
p	pressure [Pa]
P	Power [W], [HP]
PCS	Power Control System
PCU	Power Control Unit
PD	Power-Density [kW/kg], [HP/kg]
PR	Pressure Ratio [-]
SF	Safety Factor [-]
SFC	Specific Fuel Consumption [kg/W-s], [gr/HP-h]
SHP	Shaft Horse Power [kW], [HP]
SL	Sea-Level (ISA conditions)
SOC	State of Charge
STOL	Short Takeoff and Landing

TBO	Time-Between-Overhauls
TOD	Takeoff Distance [m], [ft]
TOW	Takeoff Weight/Mass [kg], [lb]
UAV	Unmanned Aerial Vehicles
VLJ	Very Light Jets
ρ	Density [kg/m^3]

REFERENCES

[1] N. E. Daidzic. 2011. Designing Propulsion Systems for Future Air/Space Transportation. Professional Pilot. 45(9): 82-86.

[2] N. E. Daidzic. 2012. FADEC Advances allow better Engine Performance. Professional Pilot. 46(3): 78-82.

[3] N. E. Daidzic. 2012. Jet Engine Thrust Ratings, Professional Pilot. 46(9): 92-96.

[4] I. Moir and A. Seabridge. 2008. Aircraft Systems - Mechanical, electrical, and avionics subsystems integration. 3rd Edition, John Wiley and Sons, Ltd., Chichester, West Sussex, England, UK.

[5] S. Farokhi. 2009. Aircraft Propulsion. John Wiley and Sons, Inc., Hoboken, NJ.

[6] C. Mikolajczak, M. Kahn, K. White and R. T. Long. 2011. Lithium-Ion Batteries Hazard and Use Assessment - Final Report, Prepared by: Exponent Failure Analysis Associates, Inc. 1100034.000 A0F0 0711 CM01, National Fire Protection Association.

[7] D. Doughty and E. P. Roth. 2012. A general discussion of Li-ion battery safety. The Electrochemical Society Interface.

[8] C. Peabody. 2011. Characterization of mechanical stress effects on lithium ion battery materials. PhD dissertation, Princeton, USA.

[9] H. Kim. 2009. Effects of mechanical stresses on lithium ion batteries. PhD dissertation, Michigan State University, USA.

[10] C. Peabody, B. Craig and C. B. Arnold. 2011. The role of mechanically induced separator creep in lithium-ion battery capacity fades. Journal of Power Sources. 196: 8147-8153.

[11] L. Piancastelli, L. Frizziero, E. Morganti, A. Canaparo: "The Electronic Stability Program controlled by a Fuzzy Algorithm tuned for tyre burst issues", Published by Pushpa Publishing House, "Far East Journal of Electronics and Communications", ISSN: 0973-7006, Volume 9, Number 1, pages 49-68, Allahabad, India, 2012.

[12] http://batteryuniversity.com/learn/article/how_to_prolong_lithium_based_batteries.

[13] S. Choi, S. Hong and H. S. Lim. 2002. Factors that affect cycle-life and possible degradation mechanisms of a Li-ion cell based on $LiCoO_2$. Journal of Power Sources. 111(1): 130-136.

[14] http://www.edn.com/design/systems-design/4391497/Teardown--High-voltage-Li-ion-battery-stack-management---the-drive-for-safe-power.

[15] L. Piancastelli, L. Frizziero, E. Morganti, A. Canaparo: "Fuzzy control system for aircraft diesel engines" edizioni ETS, "INTERNATIONAL JOURNAL OF HEAT & TECHNOLOGY", ISSN 0392-8764, Volume 30, n.1, pp. 131-135, Bologna 2012.

[16] C. Stockbridge, A. Ceruti, A. and P. Marzocca. 20120. Airship research and development in the areas of design, structures, dynamics and energy systems. International Journal of Aeronautical and Space Sciences. 13(2): 170-187.

[17] http://batteryuniversity.com/learn/article/elevating_self_discharge/.

[18] G. M. Ehrlich. 2010. Lithium-Ion Batteries, in Handbook of Batteries, 4th Edition, ed. by D. Linden and T. B. Redd, McGraw-Hill, USA.

[19] C. W. Kamienski, D. P. McDonald and M. W. Stark. 1995. Lithium and Lithium compounds, in Kirk-Othmer Encyclopedia of Chemical Technology, 4th Ed. 15 (Wiley, 1995), pp. 434-463.

[20] L. Piancastelli, L. Frizziero, I. Rocchi. 2012. An innovative method to speed up the finite element analysis of critical engine components. International Journal of Heat and Technology. 30(2): 127-132.

[21] B. Georgi, S. Hunkert, J. Liang and M. Willmann. 1997. Realizing Future Trends in Diesel Engine Development. Volkswagen AG, SAE972686.

[22] P. G. Hill and C. P. Peterson. 1992. Mechanics and Thermodynamics of Propulsion. 2nd Edition, Addison-Wesley Publishing Company, Inc., Reading.

[23] J. D. Mattingly. 2005. Elements of Gas Turbine Propulsion, AIAA Education Series. American Institute for Aeronautics and Astronautics, Reston, VA.

[24] P. J. Swatton. 2008. Aircraft Performance: Theory and Practice for Pilots, 2nd Edition. John Wiley and Sons, Chichester, West Sussex, England, UK.

[25] L. Piancastelli. and M. Pellegrini. 2007. The bonus of aircraft piston engines, an update of the Meredith effect. Int. Jour Heat and Technology. 25(2).

[26] http://www.roadandtrack.com/racing/kers-are comingagain.

[27] G. M. Saggiani, G. Caligiana and F. Persiani. 2004. Multiobjective wing design using genetic algorithm and fuzzy logic, Part G: Jour. of Aerospace Engineering. 218(2): 133-145.

[28] L. Piancastelli, L. Frizziero, S. Marcoppido, A. Donnarumma and E. Pezzuti. 2011. Active antiskid system for handling improvement in motorbikes controlled by fuzzy logic. International Journal of Heat and Technology. 29(2): 95-101.

[29] L. Piancastelli, L. Frizziero, S. Marcoppido, A. Donnarumma and E. Pezzuti. 2011. Fuzzy control system for recovering direction after spinning. International Journal of Heat and Technology. 29(2): 87-93.

[30] L. Piancastelli, L. Frizziero, S. Marcoppido and E. Pezzuti. 2012. Methodology to evaluate aircraft piston engine durability. International Journal of Heat and Technology. 30(1): 89-92.

[31] L. Piancastelli, L. Frizziero and I. Rocchi. 2012. Feasible optimum design of a turbocompound Diesel Brayton cycle for diesel-turbo-fan aircraft propulsion. International Journal of Heat and Technology. 30(1): 121-126.

[32] http://adg.stanford.edu/aa241/performance/takeoff.html.

[33] B. W. McCormick. 1995. Aerodynamics, Aeronautics and Flight Mechanics. 2nd Edition, John Wiley and Sons, Inc., New York, USA.

[34] L. Piancastelli, L. Frizziero, G. Zanuccoli, N. E. Daidzic, I. Rocchi, "A comparison between cfrp and 2195-fsw for aircraft structural designs" edizioni ETS, "International journal of heat & technology", ISSN 0392-8764, Volume 31, n.1, pp. 17-24, Bologna 2013.

[35] L. Piancastelli, N. E. Daidzic, L. Frizziero, I. Rocchi, "Analysis of automotive diesel conversions with kers for future aerospace applications" edizioni ETS, "International journal of heat & technology", ISSN 0392-8764, Volume 31, n.1, pp. 143-154, Bologna 2013.L. Frizziero, I. Rocchi: "New finite element analysis approach", Published by Pushpa Publishing House, "Far East Journal of Electronics and Communications", ISSN: 0973-7006, Volume 11, Issue 1, December 2013, pages 85-100, Allahabad, India, 2012.

[36] L. Piancastelli, L. Frizziero, E. Pezzuti, "Aircraft diesel engines controlled by fuzzy logic", Asian Research Publishing Network (ARPN), "Journal of Engineering and Applied Sciences", ISSN 1819-6608, Volume 9, Issue 1, pp. 30-34, 2014, EBSCO Publishing, 10 Estes Street, P.O. Box 682, Ipswich, MA 01938, USA.